

Unearthing the soil carbon food web with high resolution DNA-SIP

Ashley N Campbell and Charles Pepe-Ranney * † ‡, Chantal Koechli, Sean Berthrong, and Daniel H Buckley ‡

* These authors contributed equally to the manuscript and should be considered co-first authors, † Department of Microbiology, Cornell University, New York, USA, and ‡ Department of Crop and Soil Sciences, Cornell University, New York, USA

Submitted to Proceedings of the National Academy of Sciences of the United States of America

Abstract

We identify microorganisms participating in the transformation of xylose or cellulose in soil microcosms by using nucleic acid stable isotope probing (SIP) coupled to next generation sequencing. Microcosms were incubated with ^{13}C -xylose or ^{13}C -cellulose and microcosm DNA was interrogated for ^{13}C -incorporation at days 1, 3, 7, 14 and 30. A total of 49 and 63 unique OTUs assimilated ^{13}C from xylose and cellulose into DNA, respectively. Incorporation of ^{13}C from xylose into microcosm DNA was observed at days 1, 3, and 7, while incorporation of ^{13}C from cellulose peaked at day 14 and was maintained at day 30. Importantly, many cellulose degraders identified in this study are members of cosmopolitan but physiologically uncharacterized soil microbial lineages including *Sphingobacteriia*, *Chloroflexi* and *Planctomycetes*. ^{13}C -xylose additions precipitated a temporal cascade of ^{13}C -incorporation activity that could be due to significant predatory interactions among bacteria yet intra-bacteria predatory interactions are rarely considered in soil C cycling conceptual models. Microorganisms that assimilated ^{13}C -xylose were faster growing and displayed less substrate specificity than microorganisms that incorporated ^{13}C from cellulose as assessed by predicted *rrn* gene copy number for each OTU and OTU DNA buoyant density shifts in response to ^{13}C -labeling. Also, microorganisms that assimilated ^{13}C from xylose were phylogenetically overdispersed whereas ^{13}C -cellulose assimilating microorganisms were phylogenetically constrained. Describing the ecology and identities of soil C cycling microorganisms will calibrate and inform predictions of terrestrial carbon flux in response to climate change and land management. Tuning terrestrial C flux models with appropriate parameters for soil biomass is crucial for reconciling contrasting predictions of soil as a future C sink and source.

monolayer | structure | x-ray reflectivity | molecular electronics

Abbreviations: SAM, self-assembled monolayer; OTS, octadecyl-
50 trichlorosilane

Significance

We have limited understanding of soil carbon (C) cycling yet soil contains a large fraction of the global C pool. Microorganisms mediate most soil C cycling but have proven difficult to study due to the complexity of soil C biochemistry and the wide range of soil microorganisms participating in C reactions. We demonstrate C use dynamics by soil microbial taxa. Furthermore, we identified novel microorganisms involved in cellulose decomposition, the most globally abundant biopolymer. Further application of the method demonstrated in this paper will identify microbial taxa that mediate soil C transformations for more substrates and soils and increase our understanding of global soil C cycling.

Introduction

Excluding plant biomass, there are 2,300 Pg of carbon (C) stored in soils worldwide which accounts for ~80% of the global terrestrial C pool [1, 2]. When organic C from plants reaches soil it is degraded by fungi, archaea, and bacteria. The majority of plant biomass C in soil is respired and produces 10 times more CO₂ annually than anthropogenic emissions [3]. Global changes in atmospheric CO₂, temperature, and ecosystem nitrogen inputs are expected to impact soil C input [4]. Current climate change models concur on atmospheric and oceanic but not terrestrial C predictions [5]. Contrasting terrestrial C model predictions reflect how little is known about soil C cycling. Inconsis-

Reserved for Publication Footnotes

tencies in terrestrial modeling could be improved by elucidating the relationship between dissolved organic C and soil microbial community composition [6].

To establish the relationship between community structure and soil function we must identify the *in situ* activity of specific soil microbes [7]. An estimated 80–90% of soil C cycling is mediated by microorganisms [8, 9] but exploring soil C processing is challenging due to soil’s heterogeneous nature. The majority of microorganisms resist cultivation in the laboratory. Stable-isotope probing (SIP) links genetic identity and activity without cultivation and has been used to expand our knowledge of microbial contributions to biogeochemical processes [10]. Successful applications of SIP have identified organisms which mediate processes performed by a narrow set of functional guilds such as methanogens [11] but SIP has been less applicable in soil C cycling studies due to limitations in resolving power as a result of simultaneous labeling of many different organisms. High throughput DNA sequencing technology, however, has enabled exploration of complex soil C-cycling patterns via SIP.

A temporal activity cascade occurs in natural microbial communities during plant biomass degradation in which labile C is degraded before polymeric C [12, 13]. This study’s aim was to observe C assimilation dynamics in the soil microbial community. Our experimental approach included the addition of a soil organic matter (SOM) simulant to soil microcosms where a single C component was substituted for its ^{13}C equivalent. Parallel incubations of soils amended with this C mixture allowed us to observe how different C substrates move through the soil microbial community. In this study we used ^{13}C -xylose and ^{13}C -cellulose as a proxy for labile and polymeric C, respectively, and coupled nucleic acid SIP with high throughput DNA sequencing. Amplicon sequencing of 16S rRNA genes from gradient fractions of multiple density gradients made it possible to track C assimilation by hundreds of soil taxa.

Results

We observed C use dynamics in an agricultural soil microbial community by conducting a nucleic acid SIP experiment wherein xylose or cellulose carried the isotopic label. We set up three soil microcosm series (Figure XX). Each microcosm was amended with a C substrate mixture that included cellulose and xylose. The C substrate mixture approximated the C composition of fresh plant biomass. The same mixture was added to all microcosms, however, for each series except the control, xylose or cellulose was substituted for its ^{13}C

counterpart. Microcosms are identified in figures by the following code: “13CXPS” refers to the amendment with ^{13}C -xylose (**^{13}C Xylose Plant Simulant**), “13CCPS” refers to the ^{13}C -cellulose amendment and “12CCPS” refers to the amendment that only contained ^{12}C (i.e. control). 5.3 mg C substrate mixture per gram of soil was added to each microcosm representing 18% of the soil C. The mixture included 0.42 mg xylose-C and 0.88 mg cellulose-C per gram soil. Microcosms were harvested at days 1, 3, 7, 14 and 30 during a 30 day incubation. ^{13}C -xylose assimilation peaked immediately and tapered over the 30 day incubation whereas ^{13}C -cellulose assimilation peaked two weeks after amendment additions (Figure 1, Figure S1). See Supplemental Note XX for sequencing and density fractionation statistics.

Soil microcosm microbial community changes with time. Changes in the bulk soil microcosm microbial community structure and membership correlated significantly with time (Figure S2, p-value 0.23, R^2 0.63, Adonis test [14]). The identity of the ^{13}C -labeled substrate added to the microcosms did not significantly correlate with bulk soil community structure and membership (p-value 0.35). Additionally, microcosm beta diversity was significantly less than gradient fraction beta diversity (Figure S2, p-value 0.003, “betadisper” function R Vegan package [15, 16]). Twenty-nine OTUs significantly changed in relative abundance with time (“BH” adjusted p-value <0.10, [17]) and of these 29 OTUs, 14 were found to incorporate ^{13}C from labeled substrates into biomass (Figure S3). Four classes significantly (adjusted P-value <0.10) changed in abundance: *Bacilli* (decreased), *Flavobacteria* (decreased), *Gammaproteobacteria* (decreased) and *Herpetosiphonales* (increased) (Figure S4). Abundances grouped at phylum level for OTUs that incorporated ^{13}C from cellulose increased with time whereas abundances grouped at the phylum level of OTUs that incorporated ^{13}C from xylose decreased over time although *Proteobacteria* abundance spiked at day 14 (Figure S5).

OTUs that assimilated ^{13}C into DNA. Within the first 7 days of incubation 63% of ^{13}C -xylose was respired and only 6% more was respired from day 7 to 30. At day 30, 30% of the ^{13}C from xylose remained in the soil. An average 16% of the ^{13}C -cellulose added was respired within the first 7 days, 38% by day 14, and 60% by day 30.

We refer to OTUs that putatively incorporated ^{13}C into DNA originally from an isotopically labeled substrate as substrate “responders” (see Supplemental Note XX for operational “response” criteria). There were X, X, X, X, and X ^{13}C -xylose

responders at days 1, 3, 7, 14, 30, respectively (Figure S1). The numerically dominant ^{13}C -xylose responder phylum shifted from *Firmicutes* to *Bacteroidetes* and then to *Actinobacteria* across days 1, 3 and 7 (Figure 2, Figure 3). *Proteobacteria* ^{13}C -xylose responders were found at days 1, 3, 7 but peaked at day 7 (Figure 3).

Only 2 and 5 OTUs had incorporated ^{13}C from ^{13}C -cellulose at days 3 and 7, respectively. At days 14 and 30, 42 and 39 OTUs incorporated ^{13}C from ^{13}C -cellulose into biomass (Figure S1). *Proteobacteria*, *Verrucomicrobia*, and *Chloroflexi* had relatively high numbers of responders with strong response across multiple time points (Figure 2). *Verrucomicrobia* ^{13}C -cellulose responders were XX% *Spartobacteria*. *Chloroflexi* responders were annotated belonging to the *Herpetosiphonales* and XX. *Cellvibrio* a canonical soil cellulose degrader was found to respond strongly in the microcosms to ^{13}C -cellulose. See Supplemental Note XX for further analysis of ^{13}C -responsive OTUs at greater taxonomic resolution.

Ecological strategies of ^{13}C responders. ^{13}C -xylose responders are generally more abundant members based on relative abundance in bulk DNA SSU rRNA gene content than ^{13}C -cellulose responders (Figure 4, p-value 0.00028, Wilcoxon Rank Sum test). However, both abundant and rare OTUs responded to ^{13}C -xylose and ^{13}C -cellulose (Figure 4). Two ^{13}C -cellulose responders were not found in any bulk samples (“OTU.862” and “OTU.1312”, Table S1). Of the 10 most abundant responders, 8 are ^{13}C -xylose responders and 6 of these 8 are consistently among the 10 most abundant OTUs in bulk samples.

Cellulose responders exhibited a greater shift in buoyant density (BD) than xylose responders in response to isotope incorporation (Figure S6, Figure 4, p-value 1.8610×10^{-6} , Wilcoxon Rank Sum test). ^{13}C -cellulose responders shifted on average 0.0163 g mL^{-1} (sd 0.0094) whereas xylose responders shifted on average 0.0097 g mL^{-1} (sd 0.0094). For reference, 100% ^{13}C DNA BD is 0.04 g mL^{-1} greater than the BD of its ^{12}C counterpart. DNA BD increases as its ratio of ^{13}C to ^{12}C increases. An organism that only assimilates C into DNA from a ^{13}C isotopically labeled source, will have a greater $^{13}\text{C}:^{12}\text{C}$ ratio in its DNA than an organism utilizing a mixture of isotopically labeled and unlabeled C sources (see Supplemental Note XX). We predicted the *rrn* gene copy number for each OTU as described previously CITE. ^{13}C -xylose responder estimated *rrn* gene copy number was inversely related time of first response (p-value 2.02×10^{-15} , Figure S7). OTUs that first respond at later time

points have fewer estimated *rrn* copy number than OTUs that first respond earlier (Figure S7).

We assessed phylogenetic clustering of ^{13}C -responsive OTUs with the Nearest Taxon Index (NTI) and the Net Relatedness Index (NRI). Briefly, positive NRI and NTI with corresponding low P-values indicates deep phylogenetic clustering whereas negative NRI with high P-values indicates taxa are overdispersed against the null model CITE. NRI and P-values for substrate responder groups suggest ^{13}C -xylose responders are overdispersed (NRI: -1.33, P: 0.90) while cellulose responders are clustered (NRI: 4.49, P: 0.001). Nearest taxon indices (NTI) show that both ^{13}C -cellulose and ^{13}C -xylose responders are clustered near the tips of the tree (NTI: 1.43 (P: 0.072), 2.69 (P: 0.001), respectively).

Discussion

Pure culture based studies have historically driven soil microbial ecology research but culturing has not captured *in situ* numerically abundant soil genera [18]. DNA-SIP can characterize functional roles for thousands of phylotypes in a single experiment without cultivation. We identified 104 OTUs in an agricultural soil that incorporated ^{13}C from xylose and/or cellulose into biomass and characterized substrate specificity and C-cycling dynamics for these OTUs. ^{13}C -xylose and ^{13}C -cellulose responsive OTUs included members of cosmopolitan yet functionally uncharacterized soil phylogenetic groups such as *Verrucomicrobia*, *Planctomycetes* and *Chloroflexi*.

Microbial response to isotopic labels. We propose that C added to soil microcosms in this experiment took the following path through the microbial food web (Figure S8): Labile C such as xylose was first assimilated by fast-growing opportunistic *Firmicutes* aerobic spore formers. The remaining labile C biomass C from growing *Firmicutes* was assimilated in succession by *Bacteroidetes*, *Actinobacteria* and *Proteobacteria* phylotypes that were tuned to lower C substrate concentrations, were predatory bacteria (e.g. *Agromyces*), and/or were specialized for consuming viral lysate. C from polymeric substrates was decomposed by bacteria after 14 days. Canonical cellulose degrading bacteria such as *Cellvibrio* degraded cellulose but uncharacterized lineages in the *Chloroflexi*, *Planctomycetes* and *Verrucomicrobia*, specifically the *Spartobacteria*, were also significant contributors to cellulose decomposition.

Ecological strategies of soil microorganisms participating in the decomposition of organic matter. We assessed the ecology of ^{13}C -responsive OTUs

by estimating each OTU’s the *rrn* gene copy number and the BD shift upon ¹³C-labeling. *rrn* gene copy number correlates positively with growth rate [19] and BD shift is indicative of substrate specificity (see results). Ecological metrics predict ¹³C-cellulose responsive OTUs grow slower (Figure 4, Figure S7), have greater substrate specificity (Figure 4), and are generally lower abundance members of the bulk community than ¹³C-xylose responsive OTUs (Figure 4). The higher abundance of xylose responders may also be in part due to higher *rrn* gene copy number. ¹³C-xylose responsive OTUs that responded beginning at day 3 had greater *rrn* gene copy number than OTUs that responded to ¹³C-xylose later (Figure 4, Figure S7) suggesting fast-growing microbes assimilated ¹³C from xylose before slow growers.

NRI values are useful metrics for assessing phylogenetic clustering [20] and have recently been used to assess clustering of soil OTUs categorized by response to wet up [21, 22]. To our knowledge assessing the phylogenetic clustering of OTUs found to incorporate heavy isotopes into biomass during SIP incubations has not been attempted. We found that cellulose and xylose responders are clustered and overdispersed, respectively. This suggests that the ability to degrade cellulose is phylogenetically conserved possibly reflecting the complexity of cellulose degradation biochemistry. The positive relationship with a physiological trait’s phylogenetic depth and complexity has been noted previously [23] and the ¹³C-cellulose response trait depth observed in this study (X.XX 16S rRNA gene sequence divergence) is on the same order as that observed for glycoside hydrolases which are diagnostic enzymes in cellulose degradation [24]. Overdispersion, as we saw for the ¹³C-xylose responsive OTUs, may be indicative of a trait that can be transferred between species via horizontal gene transfer and/or a trait that is broadly distributed phylogenetically. It’s not clear, though, if all ¹³C-xylose responsive organisms were labeled as a result of primary xylose assimilation (see below), and therefore it’s not clear if ¹³C-xylose responsive OTUs in this experiment constitute a single ecologically meaningful group or multiple ecological groups.

Implications for soil C cycling models. Land management, climate, pollution and disturbance can all influence soil community composition [25] which in turn can influence soil biogeochemical process rates (e.g. [26]). Assessing functional group diversity and establishing identities of functional group members is necessary to predict how biogeochemical process rates can change with community composition [25, 27]. Biogeochemical processes carried out by few taxa or “narrow” guilds are influ-

enced more significantly by changes in community composition than processes carried out by greater numbers of taxa [25, 27]. Labile and recalcitrant C decomposition are considered to be carried out by “broad” and “narrow” functional guilds, respectively [25, 27]. However, the diversity of active labile C and insoluble, polymeric C decomposers in soil has not been directly quantified. Notably, we found more OTUs responded to ¹³C-cellulose, 63, than ¹³C-xylose, 49. Also, it is possible that many ¹³C-xylose responders are predatory bacteria as opposed to primary labile C degraders (see below). The cellulose and xylose decomposer functional guilds were non-overlapping in membership and represented a small fraction of total soil community diversity (Figure 5); of 104 ¹³C-responders only 8 responded to both cellulose and xylose. Interestingly, while xylose use is undoubtedly more widely distributed among global microorganisms than the ability to degrade cellulose, the number of active xylose utilizers in our microcosms was not greater than the number of cellulose decomposers.

Both ¹³C-cellulose and ¹³C-xylose responders were largely clustered near the tips of the phylogenetic tree ($NTI > 0$) at taxonomic levels broader than the OTUs established in this study (Figure S9). Therefore ¹³C-responders can be distributed into even fewer clades than number of OTUs (Figure S9). The consenTRAIT estimate for the breadth of the xylose use trait is X.XX, for instance, while our OTUs were established at 0.03 sequence identity divergence. Active cellulose and xylose responder groups were “narrow” in that few lineages relative to total observed lineages were active participants in cellulose or xylose decomposition but there is not working quantitative definition of what constitutes “narrow” versus “broad” in the literature.

We propose two scenarios for how changes in community composition can affect C cycling based on our study. For cellulose decomposition, our results suggest that cellulose degradation is a conserved and narrowly distributed trait *in situ*. Therefore, changes in community composition could greatly influence the number of microorganisms capable of cellulose degradation per unit soil and change cellulose decomposition process rates. For xylose decomposition, on the other hand, community shifts might not change the number of xylose decomposers as it is likely many microorganisms are able to use xylose. Rather, since we observed phylogenetically and ecologically coherent groups respond to ¹³C-xylose within a time point, changes in soil community composition might shift primary xylose decomposers from one phylogenetic group to another. Process rates may not change if the number of xylose decomposers is rate limiting, but, different and phylogenetically

coherent groups of xylose decomposers may differentially allocate C resources and precipitate a different trophic cascade thus influencing soil C fate if not dynamics.

The activity succession from *Firmicutes* to *Bacteroidetes* and finally *Actinobacteria* in response to ¹³C-xylose addition is a trophic cascade and/or the manifestation of the activity of functional groups tuned to different resource concentrations. *Actinobacteria* (e.g. *Agromyces*) and *Bacteroidetes* have been previously implicated as predatory soil bacteria [28, 29], however, and the activity peak of *Bacteroidetes* and *Actinobacteria* occurred with a corresponding decrease in *Firmicutes* ¹³C-xylose responder relative abundance. Considering that *Agromyces* and certain *Bacteroidetes* types are likely soil predators one parsimonious hypothesis for ¹³C-labelling of *Bacteroidetes* and *Actinobacteria* with a corresponding decrease in abundance of ¹³C-labeled *Firmicutes* is that the *Bacteroidetes* and *Actinobacteria* fed on ¹³C-labeled *Firmicutes*. If the temporal dynamics of ¹³C-xylose incorporation are due to trophic interactions, many, if not most, fast-growing labile C degraders were consumed by predatory bacteria. Hence, predatory interactions between soil bacteria may be of importance for modelling soil C turnover though intrabacteria trophic interactions in soil C cycling are rarely considered (e.g. [30]).

Conclusion. Microorganisms sequester atmospheric C and respire SOM influencing climate change on a global scale but we do not know which microorganisms carry out specific soil C transformations. In this experiment microbes from physiologically uncharacterized but ubiquitous soil lineages participated in cellulose decomposition. Cellulose C degraders included members of the *Verrucomicrobia* (*Spartobacteria*), *Chloroflexi*, *Bacteroidetes* and *Planctomycetes*. *Spartobacteria* in particular are globally cosmopolitan soil microorganisms and are often the most abundant *Verrucomicrobia* order in soil [31]. Our results also suggest that members of the *Bacteroidetes* and *Actinobacteria* act in the cascade of labile, soluble C through soil trophic levels possibly as predators. NEEDS A FINAL SENTENCE.

Methods

Additional information on sample collection and analytical methods is provided in SI Materials and Methods.

Twelve soil cores (5 cm diameter x 10 cm depth) were collected from six random sampling locations within an organically managed agricultural field in Penn Yan, New York. Soils were pretreated by sieving (2 mm), homogenizing sieved soil, and pre-incubating 10 g of dry soil weight in flasks for 2

weeks. Soils were amended with a 5.3 mg g soil⁻¹ carbon mixture; representative of natural concentrations [32]. Mixture contained 38% cellulose, 23% lignin, 20% xylose, 3% arabinose, 1% galactose, 1% glucose, and 0.5% mannose by mass, with the remaining 13.5% mass composed of an amino acid (in-house made replica of Teknova C0705) and basal salt mixture (Murashige and Skoog, Sigma Aldrich M5524). Three parallel treatments were performed; (1) unlabeled control, (2) ¹³C-cellulose, (3) ¹³C-xylose (98 atom% ¹³C, Sigma Aldrich). Each treatment had 2 replicates per time point (n = 4) except day 30 which had 4 replicates; total microcosms per treatment n = 12, except ¹³C-cellulose which was not sampled at day 1, n = 10. Other details relating to substrate addition can be found in SI. Microcosms were sampled destructively (stored at -80°C until nucleic acid processing) at days 1 (control and xylose only), 3, 7, 14, and 30.

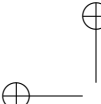
Nucleic acids were extracted using a modified Griffiths protocol [33]. To prepare nucleic acid extracts for isopycnic centrifugation as previously described [34], DNA was size selected (>4kb) using 1% low melt agarose gel and β -agarase I enzyme extraction per manufacturers protocol (New England Biolab, M0392S). For each time point in the series isopycnic gradients were setup using a modified protocol [35] for a total of five ¹²C-control, five ¹³C-xylose, and four ¹³C-cellulose microcosms. A density gradient (average density 1.69 g mL⁻¹) solution of 1.762 g cesium chloride (CsCl) mL⁻¹ in gradient buffer solution (pH 8.0 15 mM Tris-HCl, 15 mM EDTA, 15 mM KCl) was used to separate ¹³C-enriched and ¹²C-non-enriched DNA. Each gradient was loaded with approximately 5 μ g of DNA and ultracentrifuged for 66 h at 55,000 rpm and room temperature (RT). Fractions of ~100 μ L were collected from below by displacing the DNA-CsCl-gradient buffer solution in the centrifugation tube with water using a syringe pump at a flow rate of 3.3 μ L s⁻¹ [36] into AcroprepTM 96 filter plate (Pall Life Sciences 5035). The refractive index of each fraction was measured using a Reichart AR200 digital refractometer modified as previously described [34] to measure a volume of 5 μ L. Then buoyant density was calculated from the refractive index as previously described [34] (see also SI). The collected DNA fractions were purified by repetitive washing of Acroprep filter wells with TE. Finally, 50 μ L TE was added to each fraction then resuspended DNA was pipetted off the filter into a new microfuge tube.

For every gradient, 20 fractions were chosen for sequencing between the density range 1.67-1.75 g mL⁻¹. Barcoded 454 primers were designed using 454-specific adapter B, 10 bp barcodes [37], a 2 bp linker (5'-CA-3'), and 806R primer for reverse

- primer (BA806R); and 454-specific adapter A, a 2 bp linker (5'-TC-3'), and 515F primer for forward primer (BA515F). Each fraction was PCR 590 amplified using 0.25 μ L 5 U μ l⁻¹ AmpliTaq Gold (Life Technologies, Grand Island, NY; N8080243), 2.5 μ L 10X Buffer II (100 mM Tris-HCl, pH 8.3, 500 mM KCl), 2.5 μ L 25 mM MgCl₂, 4 μ L 5 mM dNTP, 1.25 μ L 10 mg mL⁻¹ BSA, 0.5 μ L 595 10 μ M BA515F, 1 μ L 5 μ M BA806R, 3 μ L H₂O, 10 μ L 1:30 DNA template) in triplicate. Samples were normalized either using Pico green quantification and manual calculation or by SequalPrepTM 600 normalization plates (Invitrogen, Carlsbad, CA; A10510), then pooled in equimolar concentrations. Pooled DNA was gel extracted from a 1% agarose 605 gel using Wizard SV gel and PCR clean-up system (Promega, Madison, WI; A9281) per manufacturer's protocol. Amplicons were sequenced 610 on Roche 454 FLX system using titanium chemistry at Selah Genomics (formerly EnGenCore, Columbia, SC)

References

1. Amundson R (2001) The carbon budget in soils. *Annu Rev Earth Planet Sci* 29(1): 535–562.
2. Batjes N-H (1996) Total carbon and nitrogen in the soils of the world. *European Journal of Soil Science* 47(2): 151–163.
3. Chapin F (2002) Principles of terrestrial ecosystem ecology.
4. Groenigen K-J, Graaff M-A, Six J, Harris D, Kuikman P, Kessel C (2006) The impact of elevated atmospheric CO₂ on soil C and N dynamics: a meta-analysis. *Managed Ecosystems and CO₂* (Springer Science, Berlin Heidelberg), pp 373–391.
5. Friedlingstein P, Cox P, Betts R, Bopp L, von W-B, Brovkin V, et al. (2006) Climate–carbon cycle feedback analysis: Results from the C4 model intercomparison. *J Climate* 19(14): 3337–3353.
6. Neff J-C, Asner G-P (2001) Dissolved organic carbon in terrestrial ecosystems: synthesis and a model. *Ecosystems* 4(1): 29–48.
7. O'Donnell A-G, Seasman M, Macrae A, Waite I, Davies J-T (2002) Plants and fertilisers as drivers of change in microbial community structure and function in soils. *Interactions in the Root Environment: An Integrated Approach* (Springer, Netherlands), pp 135–145.
8. Coleman D-C, Crossley D-A (1996) Fundamentals of Soil Ecology.
9. Nannipieri P, Ascher J, Ceccherini M-T, Landi L, Pietramellara G, Renella G (2003) Microbial diversity and soil functions. *European Journal of Soil Science* 54(4): 655–670.
10. Chen Y, Murrell J-C (2010) When metagenomics meets stable-isotope probing: progress and perspectives. *Trends Microbiol* 18(4): 157–163.
11. Lu Y (2005) In situ stable isotope probing of methanogenic archaea in the rice rhizosphere. *Science* 309(5737): 1088–1090.
12. Hu S, van Bruggen A-HC (1997) Microbial dynamics associated with multiphasic decomposition of ¹⁴C-Labeled Cellulose in Soil. *Microb Ecol* 33(2): 134–143.
13. Rui J, Peng J, Lu Y (2009) Succession of bacterial populations during plant residue decomposition in rice field soil. *Appl Environ Microbiol* 75(14): 4879–4886.
14. Anderson M-J (2001) A new method for non-parametric multivariate analysis of variance. *Austral Ecology* 26(1): 32–46.
15. Anderson M-J, Ellingsen K-E, McArdle B-H (2006) Multivariate dispersion as a measure of beta diversity. *Ecology Letters* 9(6): 683–693.
16. Oksanen J, Kindt R, Legendre P, OHara B, Stevens M-HH, Oksanen M-J, et al. (2007) The vegan package.
17. Benjamini Y, Hochberg Y (1995) Controlling the false discovery rate: a practical and powerful approach to multiple testing. *Journal of the Royal Statistical Society, Series B* 57(1): 289–300.
18. Janssen P-H (2006) Identifying the dominant soil bacterial taxa in libraries of 16S rRNA and 16S rRNA genes. *Appl Environ Microbiol* 72(3): 1719–1728.
19. Klappenbach J, Saxman P, Cole J, Schmidt T (2001) rrndb: the Ribosomal RNA Operon Copy Number Database.. *Nucleic Acids Res* 29(1): 181–184.
20. Webb C-O (2000) Exploring the phylogenetic structure of ecological communities: an example for rain forest trees.. *The American Naturalist* 156(2): 145–155.
21. Evans S-E, Wallenstein M-D (2014) Climate change alters ecological strategies of soil bacteria. *Ecol Lett* 17(2): 155–164.
22. Placella S-A, Brodie E-L, Firestone M-K (2012) Rainfall-induced carbon dioxide pulses result from sequential resuscitation of phylogenetically clustered microbial groups. *PNAS* 109(27): 10931–10936.
23. Martiny A-C, Treseder K, Pusch G (2013) Phylogenetic conservatism of functional traits in microorganisms. *ISMEJ* 7(4): 830–838.
24. Berlemont R, Martiny A-C (???) Phylogenetic distribution of potential cellulases in bacteria. *Appl Environ Microbiol* 79(5): 1545–1554.
25. McGuire K-L, Treseder K-K (2010) Microbial communities and their relevance for ecosystem models: Decomposition as a case study. *Soil*



- Biology and Biochemistry* 42(4): 529–535.
26. Berlemont R, Allison S-D, Weihe C, Lu Y, Brodie E-L, Martiny J-BH, *et al.* (2014) Cellulolytic potential under environmental changes in microbial communities from grassland litter. *Front Microbiol* 5: 639.
- 650
27. Schimel J (1995) Ecosystem consequences of microbial diversity and community structure. *Arctic and alpine biodiversity: patterns, causes and ecosystem consequences*, , eds. III P-DFSC, Körner P-DC, Ecological Studies (Springer, Berlin Heidelberg), pp 239–254.
28. Lueders T, Kindler R, Miltner A, Friedrich M-W, Kaestner M (2006) Identification of bacterial micropredators distinctively active in a soil microbial food web. *Appl Environ Microbiol* 72(8): 5342–5348.
- 655
29. Casida L-E (1983) Interaction of Agromyces ramosus with Other Bacteria in Soil. *Appl Environ Microbiol* 46(4): 881–888.
- 660
30. Moore J-C, Walter D-E, Hunt H-W (1988) Arthropod Regulation of Micro- and Meso-biota in Below-Ground Detrital Food Webs. *Annu Rev Entomol* 33(1): 419–435.
- 700
31. Bergmann G-T, Bates S-T, Eilers K-G, Lauber C-L, Caporaso J-G, Walters W-A, *et al.* (2011) The under-recognized dominance of Verrucomicrobia in soil bacterial communities. *Soil Biology and Biochemistry* 43(7): 1450–1455.
- 705
- 670
32. Schneckenberger K, Demin D, Stahr K, Kuzyakov Y (2008) Microbial utilization and mineralization of ¹⁴C glucose added in six orders of concentration to soil. *Soil Biology and Biochemistry* 40(8): 1981–1988.
33. Griffiths R-I, Whiteley A-S, O'Donnell A-G, Bailey M-J (2000) Rapid method for coextraction of DNA and RNA from natural environments for analysis of ribosomal DNA- and rRNA-based microbial community composition. *Appl Environ Microbiol* 66(12): 5488–5491.
34. Buckley D-H, Huangyutitham V, Hsu S-F, Nelson T-A (2007) Stable isotope probing with ¹⁵N achieved by disentangling the effects of genome G+C content and isotope enrichment on dna Density. *Appl Environ Microbiol* 73(10): 3189–3195.
35. Neufeld J-D, Vohra J, Dumont M-G, Lueders T, Manefield M, Friedrich M-W, *et al.* (2007) DNA stable-isotope probing. *Nature Protocols* 2(4): 860–866.
36. Manefield M, Whiteley A-S, Griffiths R-I, Bailey M-J (2002) RNA Stable isotope probing a novel means of linking microbial community function to phylogeny. *Appl Environ Microbiol* 68(11): 5367–5373.
37. Hamady M, Walker J-J, Harris J-K, Gold N-J, Knight R (2008) Error-correcting barcoded primers for pyrosequencing hundreds of samples in multiplex. *Nat Meth* 5(3): 235–237.

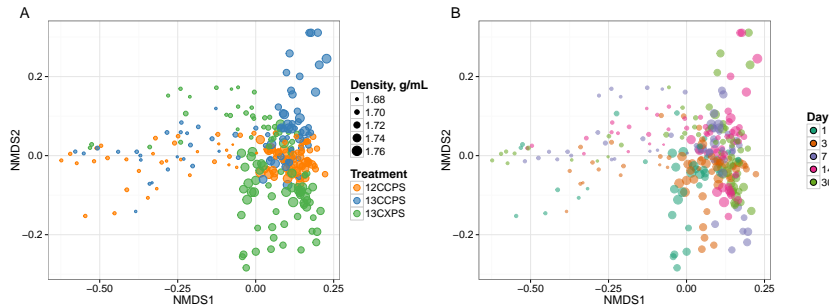


Fig. 1. NMDS analysis from weighted unifrac distances of 454 sequence data from SIP fractions of each treatment over time. Twenty fractions from a CsCl gradient fractionation for each treatment at each time point were sequenced (Fig. S1). Each point on the NMDS represents the bacterial composition based on 16S sequencing for a single fraction where the size of the point is representative of the density of that fraction and the colors represent the treatments (A) or days (B).

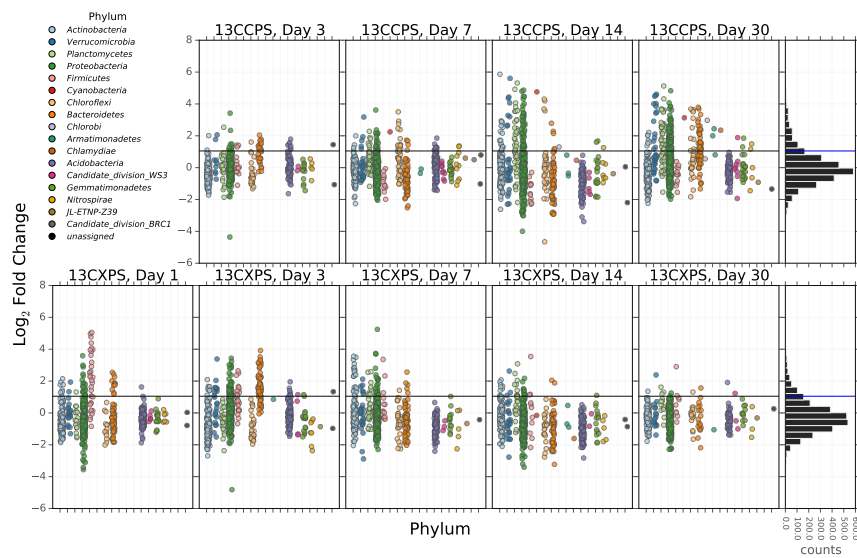


Fig. 2. Log₂ fold change of ¹³C-responders in cellulose treatment (top) and xylose treatment (bottom). Log₂ fold change is based on the relative abundance in the experimental treatment compared to the control within the density range 1.7125–1.755 g ml⁻¹. Taxa are colored by phylum. ‘Counts’ is a histogram of log₂ fold change values.

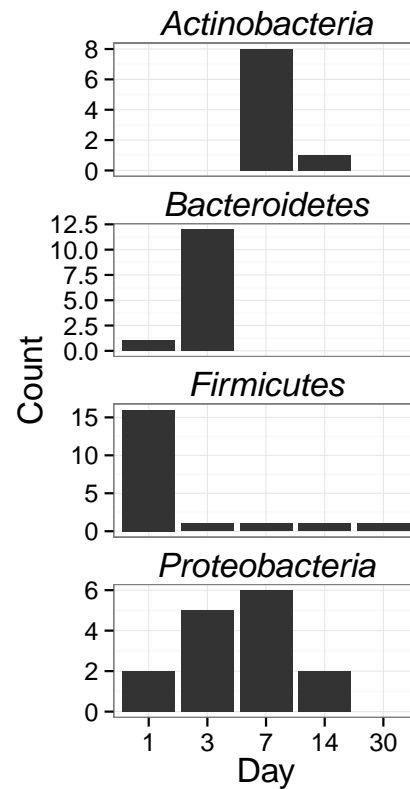


Fig. 3. Counts of ^{13}C -xylose responders in the *Actinobacteria*, *Bacteroidetes*, *Firmicutes* and *Proteobacteria* at days 1, 3, 7 and 30.

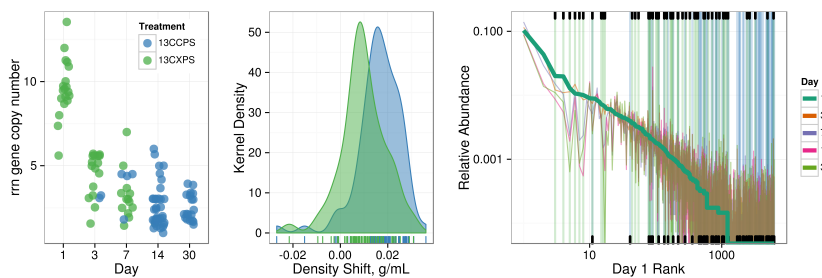


Fig. 4. ^{13}C -responder characteristics based on density shift (A) and rank (B). Kernel density estimation of ^{13}C -responder's density shift in cellulose treatment (blue) and xylose treatment (green) demonstrates degree of labeling for responders for each respective substrate. ^{13}C -responders in rank abundance are labeled by substrate (cellulose, blue; xylose, green). Ticks at top indicate location of ^{13}C -xylose responders in bulk community. Ticks at bottom indicate location of ^{13}C -cellulose responders in bulk community. OTU rank was assessed from day 1 bulk samples.

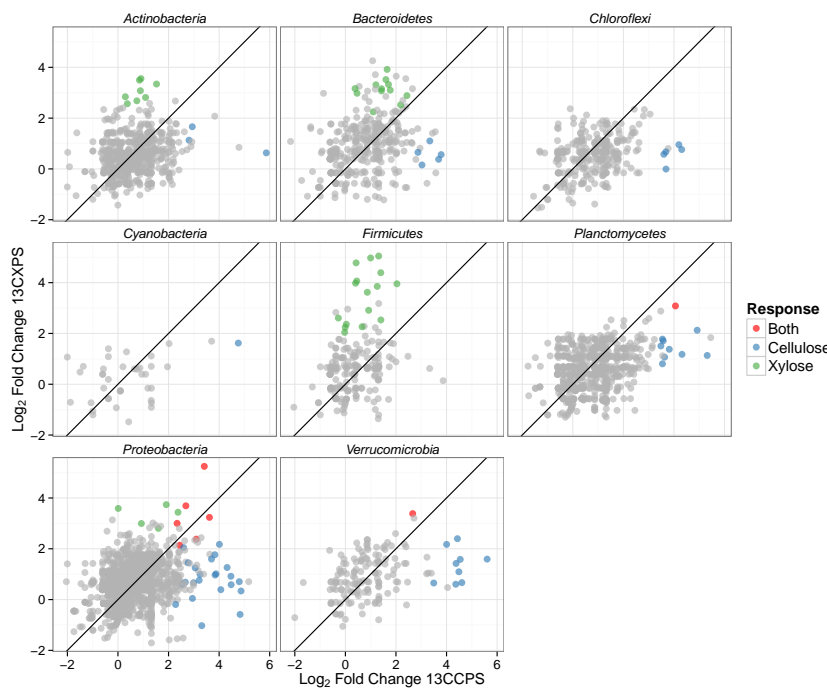


Fig. 5. Maximum log₂ fold change in response to labeled substrate incorporation for each substrate and all OTUs that pass sparsity filtering in both substrate analyses. Points colored by response. Line has slope of 1 with intercept at the origin. OTUs falling in the top-right quadrant responded to both substrates while those in the top-left and bottom-right responded to ¹³C-xylose and ¹³C-cellulose, respectively.

Supplemental Figures and Tables

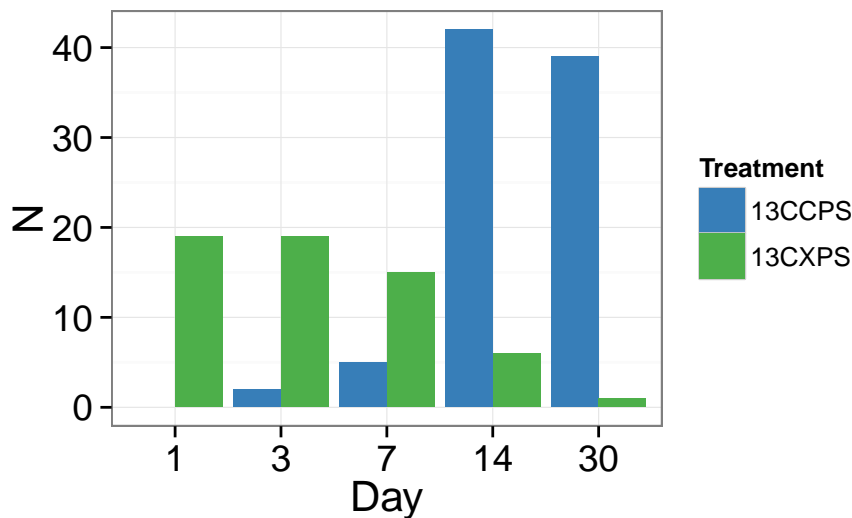


Fig. S1. Counts of responders to each isotopically labeled substrate (cellulose and xylose) over time.

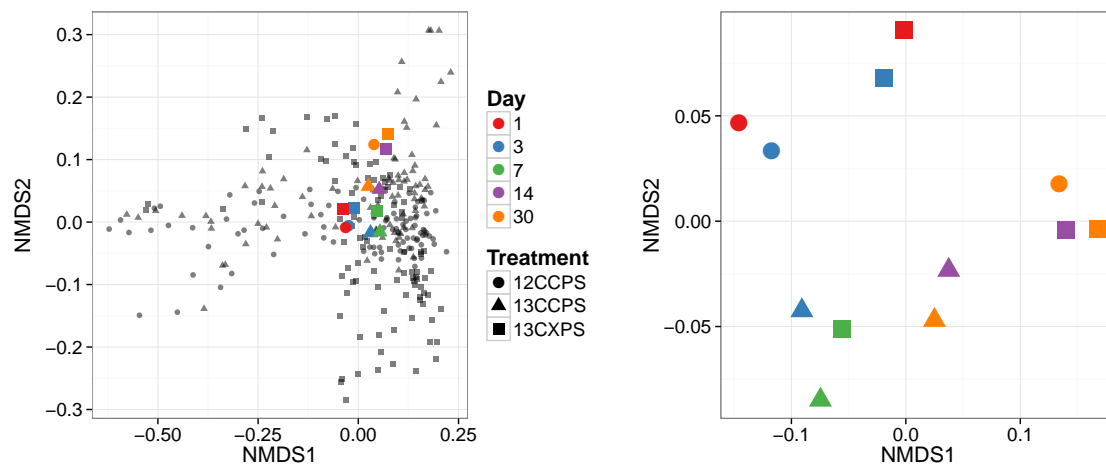


Fig. S2. Ordination of bulk gradient fraction phylogenetic profiles.

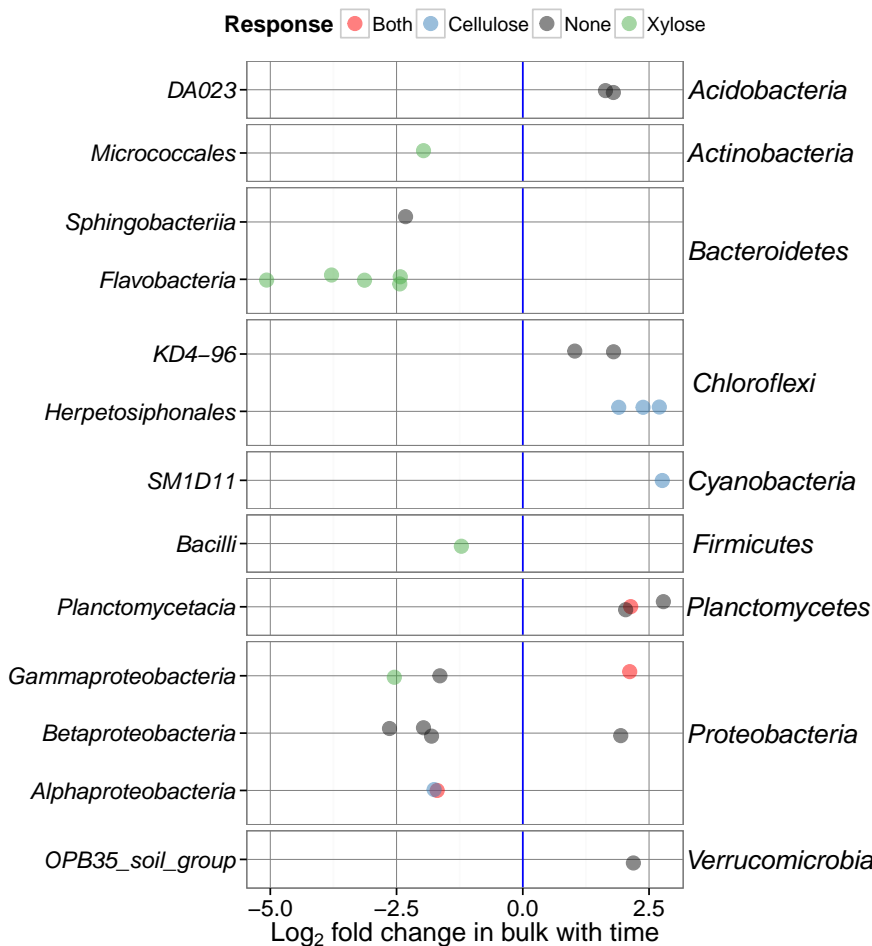


Fig. S3. Fold change time⁻¹ for OTUs that changed significantly in abundance over time. One panel per phylum (phyla indicated on the right). Taxonomic class indicated on the left.

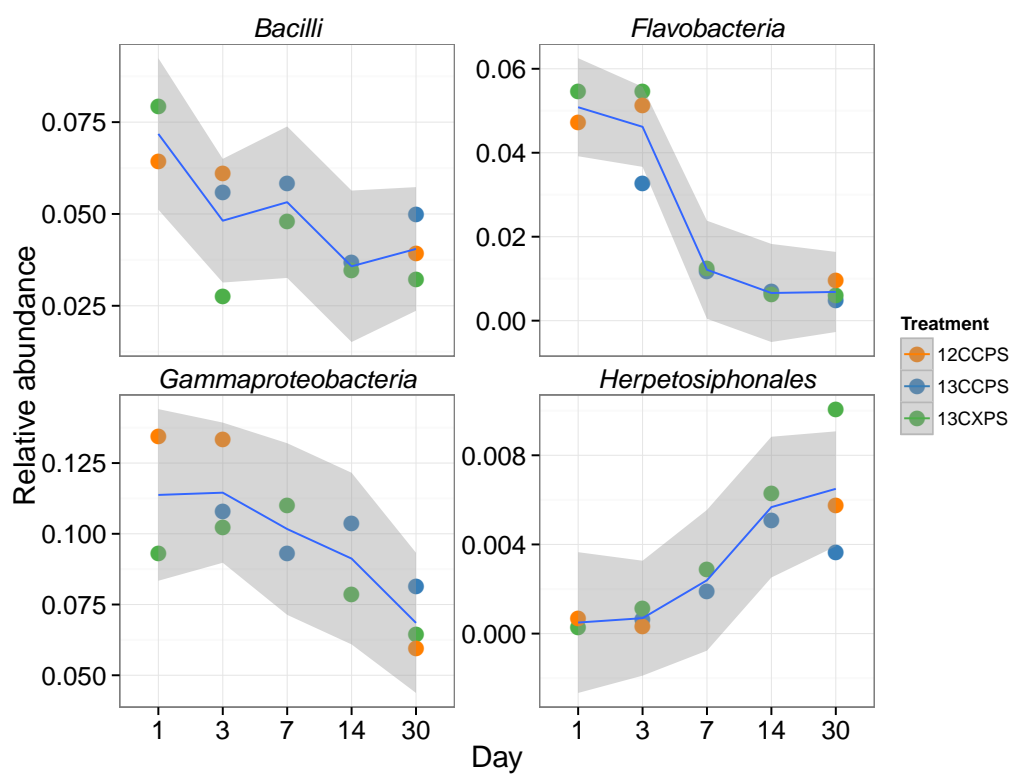
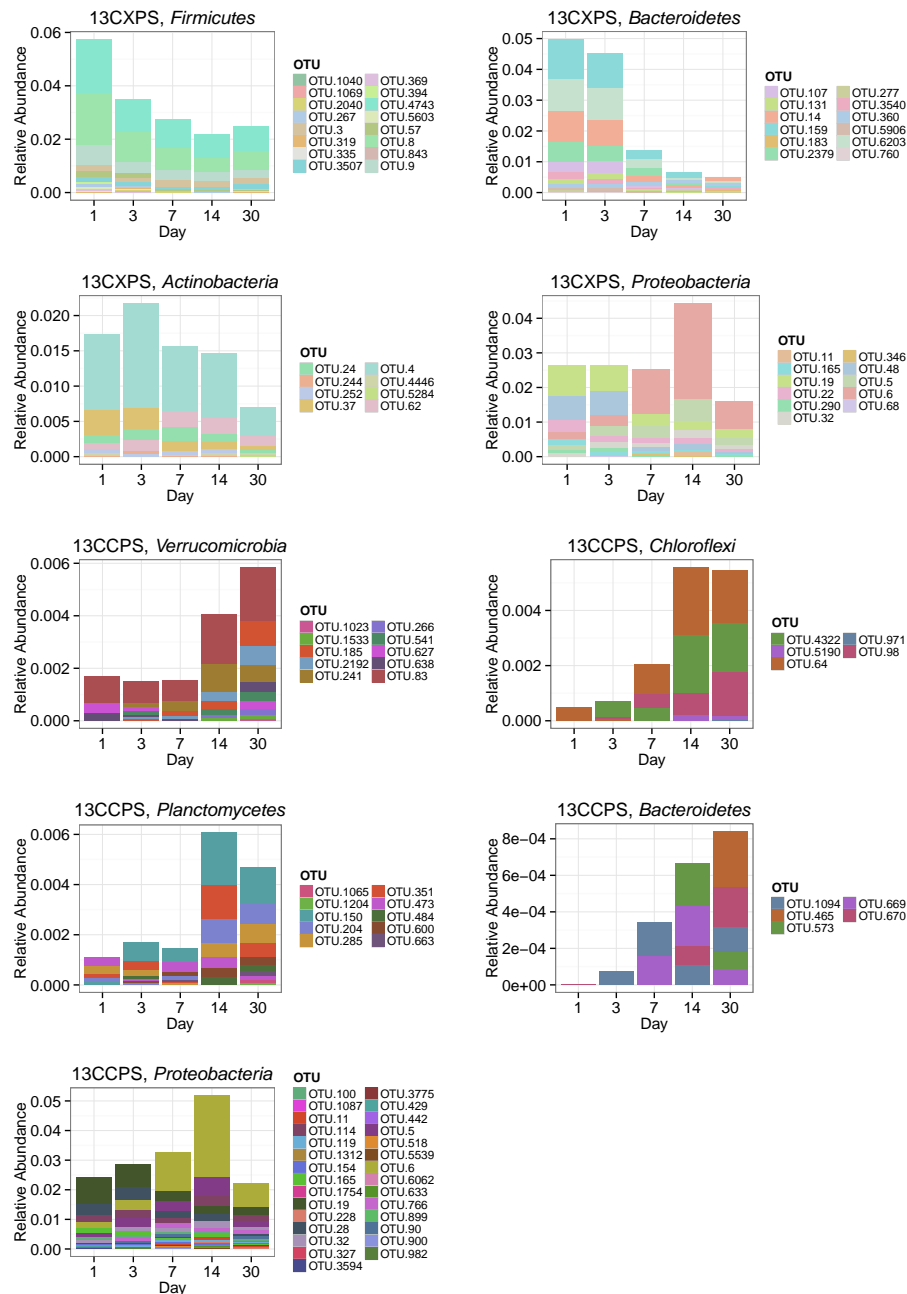


Fig. S4. Relative abundance versus day for classes that changed significantly in relative abundance with time.

**Fig. S5.** Sum of bulk abundances with selected phylum for responder OTUs.

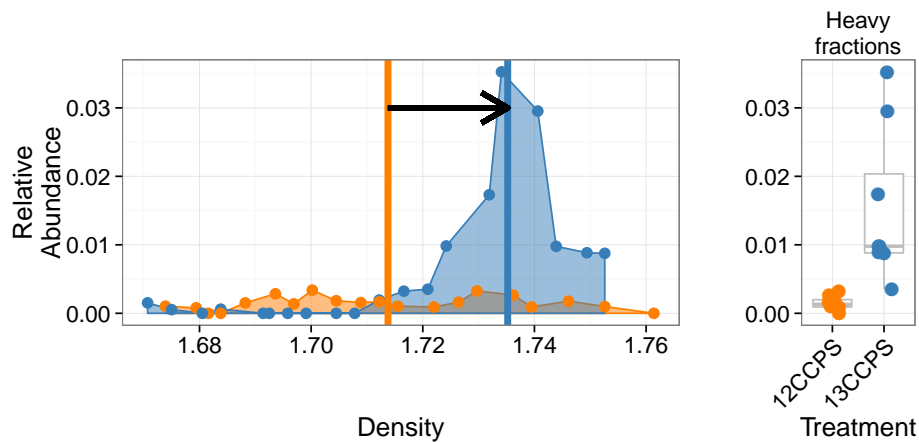


Fig. S6. Density profile for a single ^{13}C -cellulose “responder” OTU in the labeled gradient, blue, and the control gradient, orange. Vertical lines show center of mass for each density profile and arrow denotes the magnitude and direction of the BD shift upon labeling. Panel at right shows relative abundance values in the heavy fractions for each gradient.

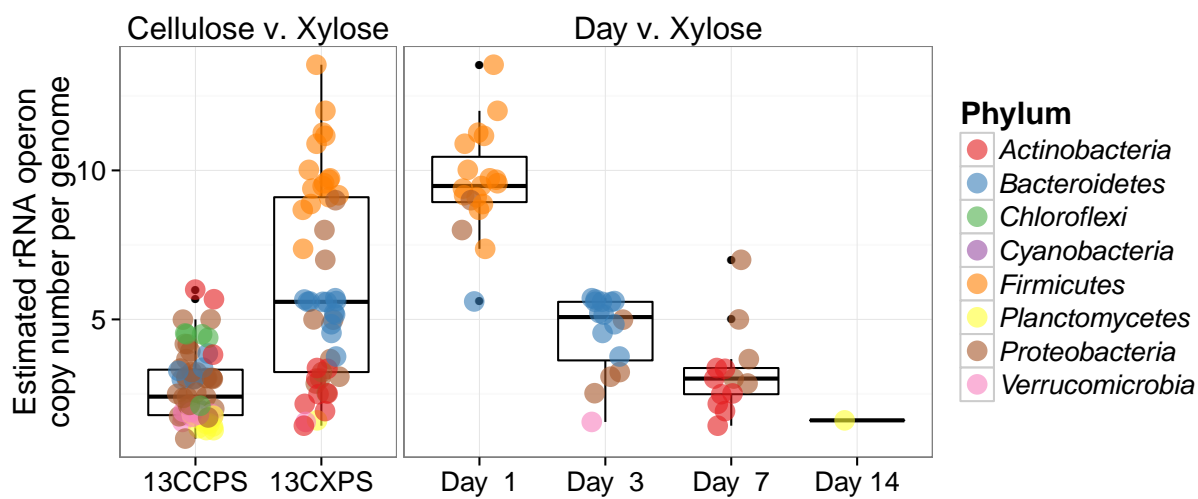


Fig. S7. Estimated rRNA operon copy number per genome for ^{13}C responding OTUs. Panel titles indicate which labeled substrate(s) are depicted.

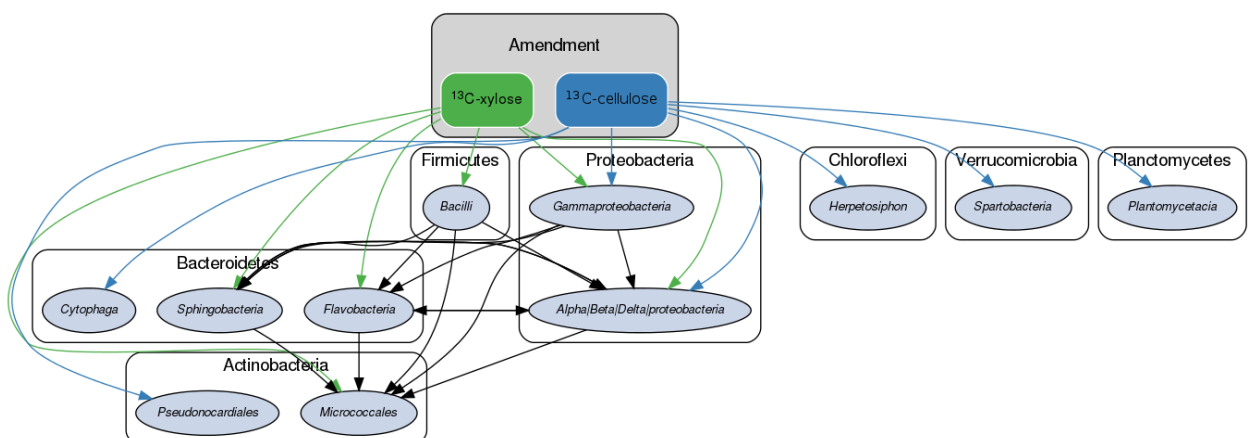


Fig. S8. Conceptual model of soil food web in this experiment. Taxa shown possessed at least two ¹³C responder OTUs for a given C substrate. *Proteobacteria* response was too varied taxonomically to depict at higher taxonomic resolution in this format. Black arrows indicate possible predator/prey interactions whereas colored arrows represent possible routes of primary degradation (green: xylose, blue: cellulose).



Fig. S9. Phylum specific trees. Heatmap indicates fold change between heavy fractions of control gradients versus labeled gradients. Dots indicate the position of “responders” to ^{13}C -xylose (green) or ^{13}C -cellulose (blue).

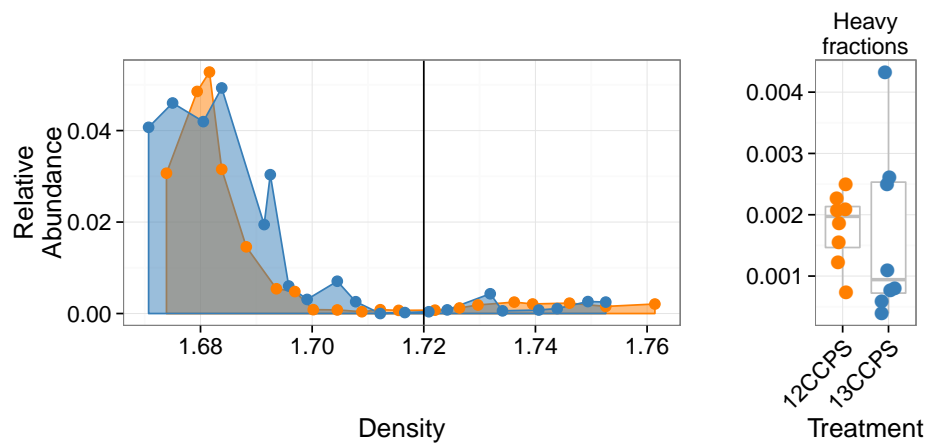


Fig. S10. Density profile for a single ^{13}C -cellulose “non-responder” OTU in the labeled gradient, blue, and the control gradient, orange. Vertical line shows where “heavy” fractions begin as defined in our analysis. Panel at right shows relative abundance values in the heavy fractions for each gradient.

Table S1: ¹³C-cellulose responders BLAST against Living Tree Project

| OTU ID | Fold change ^a | Day ^b | Top BLAST hits | BLAST %ID | Phylum;Class;Order |
|----------|--------------------------|------------------|--|-----------|--|
| OTU.100 | 2.66 | 14 | <i>Pseudoxanthomonas sacheonensis</i> , <i>Pseudoxanthomonas dokdonensis</i> | 100.0 | Proteobacteria Gammaproteobacteria Xanthomonadales |
| OTU.1023 | 4.61 | 30 | No hits of at least 90% identity | 80.54 | Verrucomicrobia Spartobacteria Chthoniobacterales |
| OTU.1065 | 5.31 | 14 | No hits of at least 90% identity | 84.55 | Planctomycetes Planctomycetacia Planctomycetales |
| OTU.1087 | 4.32 | 14 | <i>Devsia soli</i> , <i>Devsia crocina</i> , <i>Devsia riboflavina</i> | 99.09 | Proteobacteria Alphaproteobacteria Rhizobiales |
| OTU.1094 | 3.69 | 30 | <i>Sporocytophaga myxococcoides</i> | 99.55 | Bacteroidetes Cytophagia Cytophagales |
| OTU.11 | 3.41 | 14 | <i>Stenotrophomonas pavanii</i> , <i>Stenotrophomonas maltophilia</i> , <i>Pseudomonas geniculata</i> | 99.54 | Proteobacteria Gammaproteobacteria Xanthomonadales |
| OTU.114 | 2.78 | 14 | <i>Herbaspirillum sp. SUEMI03</i> , <i>Herbaspirillum sp. SUEMI10</i> , <i>Oxalicibacterium solurbis</i> , <i>Herminiumonas fonticola</i> , <i>Oxalicibacterium horti</i> | 100.0 | Proteobacteria Betaproteobacteria Burkholderiales |
| OTU.119 | 3.31 | 14 | <i>Brevundimonas alba</i> | 100.0 | Proteobacteria Alphaproteobacteria Caulobacterales |
| OTU.120 | 4.76 | 14 | <i>Vampirovibrio chlorellavorus</i> | 94.52 | Cyanobacteria SM1D11 uncultured-bacterium |
| OTU.1204 | 4.32 | 30 | <i>Planctomyces limnophilus</i> | 91.78 | Planctomycetes Planctomycetacia Planctomycetales |
| OTU.1312 | 4.07 | 30 | <i>Paucimonas lemoignei</i> | 99.54 | Proteobacteria Betaproteobacteria Burkholderiales |
| OTU.132 | 2.81 | 14 | <i>Streptomyces spp.</i> | 100.0 | Actinobacteria Streptomycetales Streptomycetaceae |
| OTU.150 | 4.06 | 14 | No hits of at least 90% identity | 86.76 | Planctomycetes Planctomycetacia Planctomycetales |
| OTU.1533 | 3.43 | 30 | No hits of at least 90% identity | 82.27 | Verrucomicrobia Spartobacteria Chthoniobacterales |
| OTU.154 | 3.24 | 14 | <i>Pseudoxanthomonas mexicana</i> , <i>Pseudoxanthomonas japonensis</i> | 100.0 | Proteobacteria Gammaproteobacteria Xanthomonadales |
| OTU.165 | 3.1 | 14 | <i>Rhizobium skieniewicense</i> , <i>Rhizobium vignae</i> , <i>Rhizobium larrymoorei</i> , <i>Rhizobium alkalisolii</i> , <i>Rhizobium galegae</i> , <i>Rhizobium huautlense</i> | 100.0 | Proteobacteria Alphaproteobacteria Rhizobiales |
| OTU.1754 | 4.48 | 14 | <i>Asticcacaulis biprosthecium</i> , <i>Asticcacaulis benevestitus</i> | 96.8 | Proteobacteria Alphaproteobacteria Caulobacterales |
| OTU.185 | 4.37 | 14 | No hits of at least 90% identity | 85.14 | Verrucomicrobia Spartobacteria Chthoniobacterales |
| OTU.19 | 2.44 | 14 | <i>Rhizobium alamii</i> , <i>Rhizobium mesosinicum</i> , <i>Rhizobium mongolense</i> , <i>Arthrobacter viscosus</i> , <i>Rhizobium sullae</i> , <i>Rhizobium yanglingense</i> , <i>Rhizobium loessense</i> | 99.54 | Proteobacteria Alphaproteobacteria Rhizobiales |
| OTU.204 | 3.81 | 14 | No hits of at least 90% identity | nan | Planctomycetes Planctomycetacia Planctomycetales |

Table S1 – continued from previous page

| OTU ID | Fold change | Day | Top BLAST hits | BLAST %ID | Phylum;Class;Order |
|----------|-------------|-----|--|-----------|---|
| OTU.2192 | 3.49 | 30 | No hits of at least 90% identity | 83.56 | Verrucomicrobia Spartobacteria Chthoniobacterales |
| OTU.228 | 2.54 | 30 | <i>Sorangium cellulosum</i> | 98.17 | Proteobacteria Deltaproteobacteria Myxococcales |
| OTU.241 | 2.66 | 14 | No hits of at least 90% identity | 87.73 | Verrucomicrobia Spartobacteria Chthoniobacterales |
| OTU.257 | 2.94 | 14 | <i>Lentzea waywayandensis</i> , <i>Lentzea flaviverrucosa</i> | 100.0 | Actinobacteria Pseudonocardiales Pseudonocardiaceae |
| OTU.266 | 4.54 | 30 | No hits of at least 90% identity | 83.64 | Verrucomicrobia Spartobacteria Chthoniobacterales |
| OTU.28 | 2.59 | 14 | <i>Rhizobium giardinii</i> , <i>Rhizobium tubonense</i> , <i>Rhizobium tibeticum</i> , <i>Rhizobium mesoamericanum CCGE 501</i> , <i>Rhizobium herbae</i> , <i>Rhizobium endophyticum</i> | 99.54 | Proteobacteria Alphaproteobacteria Rhizobiales |
| OTU.285 | 3.55 | 30 | <i>Blastopirellula marina</i> | 90.87 | Planctomycetes Planctomycetacia Planctomycetales |
| OTU.32 | 2.34 | 3 | <i>Sandaracinus amylolyticus</i> | 94.98 | Proteobacteria Deltaproteobacteria Myxococcales |
| OTU.327 | 2.99 | 14 | <i>Asticcacaulis biprosthecum</i> , <i>Asticcacaulis benevestitus</i> | 98.63 | Proteobacteria Alphaproteobacteria Caulobacterales |
| OTU.351 | 3.54 | 14 | <i>Pirellula staleyi DSM 6068</i> | 91.86 | Planctomycetes Planctomycetacia Planctomycetales |
| OTU.3594 | 3.83 | 30 | <i>Chondromyces robustus</i> | 90.41 | Proteobacteria Deltaproteobacteria Myxococcales |
| OTU.3775 | 3.88 | 14 | <i>Devosia glacialis</i> , <i>Devosia chinhatensis</i> , <i>Devosia geojensis</i> , <i>Devosia yakushimensis</i> | 98.63 | Proteobacteria Alphaproteobacteria Rhizobiales |
| OTU.429 | 3.7 | 30 | <i>Devosia limi</i> , <i>Devosia psychrophila</i> | 97.72 | Proteobacteria Alphaproteobacteria Rhizobiales |
| OTU.4322 | 4.19 | 14 | No hits of at least 90% identity | 89.14 | Chloroflexi Herpetosiphonales Herpetosiphonaceae |
| OTU.442 | 3.05 | 30 | <i>Chondromyces robustus</i> | 92.24 | Proteobacteria Deltaproteobacteria Myxococcales |
| OTU.465 | 3.79 | 30 | <i>Ohtaekwangia kribbensis</i> | 92.73 | Bacteroidetes Cytophagia Cytophagales |
| OTU.473 | 3.58 | 14 | <i>Pirellula staleyi DSM 6068</i> | 90.91 | Planctomycetes Planctomycetacia Planctomycetales |
| OTU.484 | 4.92 | 14 | No hits of at least 90% identity | 89.09 | Planctomycetes Planctomycetacia Planctomycetales |
| OTU.5 | 2.69 | 14 | <i>Delftia tsuruhatensis</i> , <i>Delftia lacustris</i> | 100.0 | Proteobacteria Betaproteobacteria Burkholderiales |
| OTU.518 | 4.8 | 14 | <i>Hydrogenophaga intermedia</i> | 100.0 | Proteobacteria Betaproteobacteria Burkholderiales |
| OTU.5190 | 3.6 | 30 | No hits of at least 90% identity | 88.13 | Chloroflexi Herpetosiphonales Herpetosiphonaceae |
| OTU.541 | 4.49 | 30 | No hits of at least 90% identity | 84.23 | Verrucomicrobia Spartobacteria Chthoniobacterales |
| OTU.5539 | 4.01 | 14 | <i>Devosia subaequoris</i> | 98.17 | Proteobacteria Alphaproteobacteria Rhizobiales |

Table S1 – continued from previous page

| OTU ID | Fold change | Day | Top BLAST hits | BLAST %ID | Phylum;Class;Order |
|----------|-------------|-----|---|-----------|--|
| OTU.573 | 3.03 | 30 | <i>Adhaeribacter aerophilus</i> | 92.76 | <i>Bacteroidetes Cytophagia Cytophagales</i> |
| OTU.6 | 3.62 | 7 | <i>Cellvibrio fulvus</i> | 100.0 | <i>Proteobacteria Gammaproteobacteria Pseudomonadales</i> |
| OTU.600 | 3.48 | 30 | No hits of at least 90% identity | 80.37 | <i>Planctomycetes Planctomycetacia Planctomycetales</i> |
| OTU.6062 | 4.83 | 30 | <i>Dokdonella sp. DC-3, Luteibacter rhizovicinus</i> | 97.26 | <i>Proteobacteria Gammaproteobacteria Xanthomonadales</i> |
| OTU.627 | 4.43 | 14 | <i>Verrucomicrobiaceae bacterium DC2a-G7</i> | 100.0 | <i>Verrucomicrobia Verrucomicrobiae Verrucomicrobiales</i> |
| OTU.633 | 3.84 | 30 | No hits of at least 90% identity | 89.5 | <i>Proteobacteria Deltaproteobacteria Myxococcales</i> |
| OTU.638 | 4.0 | 30 | <i>Luteolibacter sp. CCTCC AB 2010415, Luteolibacter algae</i> | 93.61 | <i>Verrucomicrobia Verrucomicrobiae Verrucomicrobiales</i> |
| OTU.64 | 4.31 | 14 | No hits of at least 90% identity | 89.5 | <i>Chloroflexi Herpetosiphonales Herpetosiphonaceae</i> |
| OTU.663 | 3.63 | 30 | <i>Pirellula staleyi DSM 6068</i> | 90.87 | <i>Planctomycetes Planctomycetacia Planctomycetales</i> |
| OTU.669 | 3.34 | 30 | <i>Ohtaekwangia koreensis</i> | 92.69 | <i>Bacteroidetes Cytophagia Cytophagales</i> |
| OTU.670 | 2.87 | 30 | <i>Adhaeribacter aerophilus</i> | 91.78 | <i>Bacteroidetes Cytophagia Cytophagales</i> |
| OTU.766 | 3.21 | 14 | <i>Devosia insulae</i> | 99.54 | <i>Proteobacteria Alphaproteobacteria Rhizobiales</i> |
| OTU.83 | 5.61 | 14 | <i>Luteolibacter sp. CCTCC AB 2010415</i> | 97.72 | <i>Verrucomicrobia Verrucomicrobiae Verrucomicrobiales</i> |
| OTU.862 | 5.87 | 14 | <i>Allokutzneria albata</i> | 100.0 | <i>Actinobacteria Pseudonocardiales Pseudonocardiaceae</i> |
| OTU.899 | 2.28 | 30 | <i>Enhygromyxa salina</i> | 97.72 | <i>Proteobacteria Deltaproteobacteria Myxococcales</i> |
| OTU.90 | 2.94 | 14 | <i>Sphingopyxis panaciterrae, Sphingopyxis chilensis, Sphingopyxis sp. BZ30, Sphingomonas sp.</i> | 100.0 | <i>Proteobacteria Alphaproteobacteria Sphingomonadales</i> |
| OTU.900 | 4.87 | 14 | <i>Brevundimonas vesicularis, Brevundimonas nasdae</i> | 100.0 | <i>Proteobacteria Alphaproteobacteria Caulobacterales</i> |
| OTU.971 | 3.68 | 30 | No hits of at least 90% identity | 78.57 | <i>Chloroflexi Anaerolineae Anaerolineales</i> |
| OTU.98 | 3.68 | 14 | No hits of at least 90% identity | 88.18 | <i>Chloroflexi Herpetosiphonales Herpetosiphonaceae</i> |
| OTU.982 | 4.47 | 14 | <i>Devosia neptuniae</i> | 100.0 | <i>Proteobacteria Alphaproteobacteria Rhizobiales</i> |

^a Maximum observed \log_2 of fold change.^b Day of maximum fold change.

Table S2: ^{13}C -xylose responders BLAST against Living Tree Project

| OTU ID | Fold change ^a | Day ^b | Top BLAST hits | BLAST %ID | Phylum;Class;Order |
|----------|--------------------------|------------------|--|-----------|---|
| OTU.1040 | 4.78 | 1 | <i>Paenibacillus daejeonensis</i> | 100.0 | <i>Firmicutes Bacilli Bacillales</i> |
| OTU.1069 | 3.85 | 1 | <i>Paenibacillus terrigena</i> | 100.0 | <i>Firmicutes Bacilli Bacillales</i> |
| OTU.107 | 2.25 | 3 | <i>Flavobacterium sp. 15C3</i> , <i>Flavobacterium banpakuense</i> | 99.54 | <i>Bacteroidetes Flavobacteria Flavobacteriales</i> |
| OTU.11 | 5.25 | 7 | <i>Stenotrophomonas pavanii</i> , <i>Stenotrophomonas maltophilia</i> , <i>Pseudomonas geniculata</i> | 99.54 | <i>Proteobacteria Gammaproteobacteria Xanthomonadales</i> |
| OTU.131 | 3.07 | 3 | <i>Flavobacterium fluvii</i> , <i>Flavobacterium bacterium HMD1033</i> , <i>Flavobacterium sp. HMD1001</i> | 100.0 | <i>Bacteroidetes Flavobacteria Flavobacteriales</i> |
| OTU.14 | 3.92 | 3 | <i>Flavobacterium oncorhynchi</i> , <i>Flavobacterium glycines</i> , <i>Flavobacterium succinicans</i> | 99.09 | <i>Bacteroidetes Flavobacteria Flavobacteriales</i> |
| OTU.150 | 3.08 | 14 | No hits of at least 90% identity | 86.76 | <i>Planctomycetes Planctomycetacia Planctomycetales</i> |
| OTU.159 | 3.16 | 3 | <i>Flavobacterium hibernum</i> | 98.17 | <i>Bacteroidetes Flavobacteria Flavobacteriales</i> |
| OTU.165 | 2.38 | 3 | <i>Rhizobium skieniewicense</i> , <i>Rhizobium vignae</i> , <i>Rhizobium larrymoorei</i> , <i>Rhizobium alkalisolii</i> , <i>Rhizobium galegae</i> , <i>Rhizobium huautlense</i> | 100.0 | <i>Proteobacteria Alphaproteobacteria Rhizobiales</i> |
| OTU.183 | 3.31 | 3 | No hits of at least 90% identity | 89.5 | <i>Bacteroidetes Sphingobacteriia Sphingobacteriales</i> |
| OTU.19 | 2.14 | 7 | <i>Rhizobium alamii</i> , <i>Rhizobium mesosinicum</i> , <i>Rhizobium mongolense</i> , <i>Arthrobacter viscosus</i> , <i>Rhizobium sullae</i> , <i>Rhizobium yanglingense</i> , <i>Rhizobium loessense</i> | 99.54 | <i>Proteobacteria Alphaproteobacteria Rhizobiales</i> |
| OTU.2040 | 2.91 | 1 | <i>Paenibacillus pectinilyticus</i> | 100.0 | <i>Firmicutes Bacilli Bacillales</i> |
| OTU.22 | 2.8 | 7 | <i>Paracoccus sp. NB88</i> | 99.09 | <i>Proteobacteria Alphaproteobacteria Rhodobacterales</i> |
| OTU.2379 | 3.1 | 3 | <i>Flavobacterium pectinovorum</i> , <i>Flavobacterium sp. CS100</i> | 97.72 | <i>Bacteroidetes Flavobacteria Flavobacteriales</i> |
| OTU.24 | 2.81 | 7 | <i>Cellulomonas aerilata</i> , <i>Cellulomonas humilata</i> , <i>Cellulomonas terrae</i> , <i>Cellulomonas soli</i> , <i>Cellulomonas xylinilytica</i> | 100.0 | <i>Actinobacteria Micrococcales Cellulomonadaceae</i> |
| OTU.241 | 3.38 | 3 | No hits of at least 90% identity | 87.73 | <i>Verrucomicrobia Spartobacteria Chthoniobacterales</i> |
| OTU.244 | 3.08 | 7 | <i>Cellulosimicrobium funkei</i> , <i>Cellulosimicrobium terreum</i> | 100.0 | <i>Actinobacteria Micrococcales Promicromonosporaceae</i> |
| OTU.252 | 3.34 | 7 | <i>Promicromonospora thailandica</i> | 100.0 | <i>Actinobacteria Micrococcales Promicromonosporaceae</i> |
| OTU.267 | 4.97 | 1 | <i>Paenibacillus pabuli</i> , <i>Paenibacillus tundrae</i> , <i>Paenibacillus taichungensis</i> , <i>Paenibacillus xylohexedens</i> , <i>Paenibacillus xylinilyticus</i> | 100.0 | <i>Firmicutes Bacilli Bacillales</i> |
| OTU.277 | 3.52 | 3 | <i>Solibius ginsengiterrae</i> | 95.43 | <i>Bacteroidetes Sphingobacteriia Sphingobacteriales</i> |

Table S2 – continued from previous page

| OTU ID | Fold change | Day | Top BLAST hits | BLAST %ID | Phylum;Class;Order |
|----------|-------------|-----|---|-----------|---|
| OTU.290 | 3.59 | 1 | <i>Pantoea spp.</i> , <i>Klugvera spp.</i> , <i>Klebsiella spp.</i> , <i>Erwinia spp.</i> , <i>Enterobacter spp.</i> , <i>Buttiauxella spp.</i> | 100.0 | Proteobacteria Gammaproteobacteria Enterobacterales |
| OTU.3 | 2.61 | 1 | [<i>Brevibacterium</i>] <i>frigoritolerans</i> , <i>Bacillus sp.</i> LMG 20238, <i>Bacillus coahuilensis</i> m4-4, <i>Bacillus simplex</i> | 100.0 | Firmicutes Bacilli Bacillales |
| OTU.319 | 3.98 | 1 | <i>Paenibacillus xinjiangensis</i> | 97.25 | Firmicutes Bacilli Bacillales |
| OTU.32 | 3.0 | 3 | <i>Sandaracinus amyloyticus</i> | 94.98 | Proteobacteria Deltaproteobacteria Myxococcales |
| OTU.335 | 2.53 | 1 | <i>Paenibacillus thailandensis</i> | 98.17 | Firmicutes Bacilli Bacillales |
| OTU.346 | 3.44 | 3 | <i>Pseudoduganella violaceinigra</i> | 99.54 | Proteobacteria Betaproteobacteria Burkholderiales |
| OTU.3507 | 2.36 | 1 | <i>Bacillus spp.</i> | 98.63 | Firmicutes Bacilli Bacillales |
| OTU.3540 | 2.52 | 3 | <i>Flavobacterium terrigena</i> | 99.54 | Bacteroidetes Flavobacteria Flavobacterales |
| OTU.360 | 2.98 | 3 | <i>Flavisolibacter ginsengisoli</i> | 95.0 | Bacteroidetes Sphingobacteriia Sphingobacterales |
| OTU.369 | 5.05 | 1 | <i>Paenibacillus sp.</i> D75, <i>Paenibacillus glycansilyticus</i> | 100.0 | Firmicutes Bacilli Bacillales |
| OTU.37 | 2.68 | 7 | <i>Phycicola gilvus</i> , <i>Microterricola viridarii</i> , <i>Frigeribacterium faeni</i> , <i>Frondihabitans sp.</i> RS-15, <i>Frondihabitans australicus</i> | 100.0 | Actinobacteria Micrococcales Microbacteriaceae |
| OTU.394 | 4.06 | 1 | <i>Paenibacillus pocheonensis</i> | 100.0 | Firmicutes Bacilli Bacillales |
| OTU.4 | 2.84 | 7 | <i>Agromyces ramosus</i> | 100.0 | Actinobacteria Micrococcales Microbacteriaceae |
| OTU.4446 | 3.49 | 7 | <i>Catenuloplanes niger</i> , <i>Catenuloplanes castaneus</i> , <i>Catenuloplanes atrovinosus</i> , <i>Catenuloplanes crispus</i> , <i>Catenuloplanes nepalensis</i> , <i>Catenuloplanes japonicus</i> | 97.72 | Actinobacteria Frankiales Nakamurellaceae |
| OTU.4743 | 2.24 | 1 | <i>Lysinibacillus fusiformis</i> , <i>Lysinibacillus sphaericus</i> | 99.09 | Firmicutes Bacilli Bacillales |
| OTU.48 | 2.99 | 1 | <i>Aeromonas spp.</i> | 100.0 | Proteobacteria Gammaproteobacteria aaa34a10 |
| OTU.5 | 3.69 | 7 | <i>Delftia tsuruhatensis</i> , <i>Delftia lacustris</i> | 100.0 | Proteobacteria Betaproteobacteria Burkholderiales |
| OTU.5284 | 3.56 | 7 | <i>Isopotericola nanjingensis</i> , <i>Isopotericola hypogaeus</i> , <i>Isopotericola variabilis</i> | 98.63 | Actinobacteria Micrococcales Promicromonosporaceae |
| OTU.5603 | 3.96 | 1 | <i>Paenibacillus uliginis</i> | 100.0 | Firmicutes Bacilli Bacillales |
| OTU.57 | 4.39 | 1 | <i>Paenibacillus castaneae</i> | 98.62 | Firmicutes Bacilli Bacillales |
| OTU.5906 | 3.16 | 3 | <i>Terrimonas sp.</i> M-8 | 96.8 | Bacteroidetes Sphingobacteriia Sphingobacterales |
| OTU.6 | 3.24 | 3 | <i>Cellvibrio fulvus</i> | 100.0 | Proteobacteria Gammaproteobacteria Pseudomonadales |
| OTU.62 | 2.57 | 7 | <i>Nakamurella flava</i> | 100.0 | Actinobacteria Frankiales Nakamurellaceae |

Table S2 – continued from previous page

| OTU ID | Fold change | Day | Top BLAST hits | BLAST %ID | Phylum;Class;Order |
|----------|-------------|-----|---|-----------|---|
| OTU.6203 | 3.32 | 3 | <i>Flavobacterium granuli</i> , <i>Flavobacterium glaciei</i> | 100.0 | <i>Bacteroidetes Flavobacteria Flavobacteriales</i> |
| OTU.68 | 3.74 | 7 | <i>Shigella flexneri</i> , <i>Escherichia fergusonii</i> , <i>Escherichia coli</i> , <i>Shigella sonnei</i> | 100.0 | <i>Proteobacteria Gammaproteobacteria Enterobacteriales</i> |
| OTU.760 | 2.89 | 3 | <i>Dyadobacter hamtensis</i> | 98.63 | <i>Bacteroidetes Cytophagia Cytophagales</i> |
| OTU.8 | 2.26 | 1 | <i>Bacillus niacini</i> | 100.0 | <i>Firmicutes Bacilli Bacillales</i> |
| OTU.843 | 3.62 | 1 | <i>Paenibacillus agaragedens</i> | 100.0 | <i>Firmicutes Bacilli Bacillales</i> |
| OTU.9 | 2.04 | 1 | <i>Bacillus megaterium</i> , <i>Bacillus flexus</i> | 100.0 | <i>Firmicutes Bacilli Bacillales</i> |

^a Maximum observed \log_2 of fold change.^b Day of maximum fold change.